文章编号：1000-7032(2016)02-0131-07

Luminescence of Blue-purple Emitting $Sr_2SiO_4:Ce^{3+},Li^+$ Phosphor

YOU Jing[1], XIA Li-na[1], LI Xiang-qi[1,2*], XIE Xiu-zhen[1]

(1. *College of Materials Science and Engineering, Fuzhou University, Fuzhou* 350108, *China*;
2. *Key Laboratory of Eco-materials Advanced Technology, Fuzhou University, Fuzhou* 350108, *China*)

* *Corresponding Author, E-mail: lxiangqi@fzu.edu.cn*

Abstract: Blue-purple emitting $Sr_{2-x}SiO_4:xCe^{3+}$ ($x=0.01-0.09$, in steps of 0.01) and $Sr_{1.95-y}SiO_4:0.05Ce^{3+},yLi^+$ ($y=0.01-0.07$, in steps of 0.02) phosphors have been prepared by co-precipitation method with MCM-41 as silica source. The emission spectra of $Sr_{2-x}SiO_4:xCe^{3+}$ show an asymmetric broad band with a maximum around 410 nm and the critical mole fraction is found to be 5%. Ce^{3+} ions prefer nine-coordinated Sr(Ⅱ) sites over ten-coordinated Sr(Ⅰ) sites. The emission intensity of $Sr_{1.95}SiO_4:0.05Ce^{3+}$ can be improved effectively by co-doping Li^+ ions as charge compensator and a greater degree of the improvement is observed for phosphor calcined at 1 100 ℃ compared with 1 000 ℃. The most suitable doping amount of Li^+ for $Sr_{1.95-y}SiO_4:0.05Ce^{3+},yLi^+$ is $y=0.05$.

Key words: phosphor; $Sr_2SiO_4:Ce^{3+},Li^+$; luminescence
CLC number: O482.31 **Document code**: A **DOI**: 10.3788/fgxb20163702.0131

$Sr_2SiO_4:Ce^{3+},Li^+$ 蓝紫色荧光粉发光性能的研究

游 静[1], 夏丽娜[1], 李湘祁[1,2*], 谢秀珍[1]

(1. 福州大学 材料科学与工程学院, 福建 福州 350108;
2. 福州大学 生态环境材料先进技术重点实验室, 福建 福州 350108)

摘要: 以MCM-41为硅源,采用共沉淀法制备$Sr_{2-x}SiO_4:xCe^{3+}$($x=0.01\sim0.09$,步长为0.01)和$Sr_{1.95-y}SiO_4:0.05Ce^{3+},yLi^+$($y=0.01\sim0.07$,步长为0.02)蓝紫色荧光粉。$Sr_{2-x}SiO_4:xCe^{3+}$的发射光谱是一个不对称的宽带,最大峰值在410 nm左右。Ce^{3+}的最佳掺杂量为5%。Ce^{3+}离子倾向于占据九配位的Sr(Ⅱ)格位。共掺电荷补偿剂Li^+可以有效地提高$Sr_{1.95}SiO_4:0.05Ce^{3+}$的发光强度,其中$Li^+$离子对1 100 ℃煅烧样品的发光强度的提高程度比1 000 ℃的更高,Li^+的最佳掺杂量为$y=0.05$。

关 键 词: 荧光粉; $Sr_2SiO_4:Ce^{3+},Li^+$; 发光

1 Introduction

As a new type of solid light source, white light emitting diodes (WLEDs) have attracted much attention due to high power efficiency, energy saving and environment-friendliness *etc*. Compared with the WLEDs based on yellow YAG phosphors combined with a blue InGaN LED chip, the NUV-excited

收稿日期: 2015-11-20; **修订日期**: 2015-12-08

blends of blue-, green-, and red-emitting phosphors have the higher color reproduction and color rendering[1-4]. As a good candidate excited in the NUV range, Sr_2SiO_4 matrix phosphor is extensively studied because of its good chemical stability and thermal stability[5-10].

The commonly doped rare-earth luminescent-centers in Sr_2SiO_4 matrix include Eu^{2+}, Eu^{3+}, Ce^{3+}, Dy^{3+}, *etc.* $Sr_2SiO_4:Eu^{2+}$ is one of the prevailing green-yellow phosphors for WLEDs[8]. $Sr_{1.97-(x+y)}Dy_{0.03}Ce_xLi_ySiO_4$ can emit colour from blue-white to orange-white by varying Dy^{3+} concentration[9]. The non-equivalent substitution of divalent ion by trivalent ion would create vacancies, which quench the luminescence. Reports show that co-doping of charge compensator (Li^+, Na^+, K^+) can solve this problem and enhance the emission intensities of phosphors, such as $Sr_2SiO_4:Tb^{3+}$[10], $Sr_3B_2O_6:Ce^{3+},Eu^{2+}$[11], $(Ba_{1-x}Sr_x)_9Sc_2Si_6O_{24}:Ce^{3+}$[12], and $Sr_2SiO_4:Sm^{3+}$[13]. In addition to charge compensator, the luminescence of rare-earth ions doped Sr_2SiO_4 is also influenced by the local coordination of the rare-earth ions in the host lattice. Sr_2SiO_4 exists in two crystalline phases: β-Sr_2SiO_4 (monoclinic) and α′-Sr_2SiO_4 (orthorhombic). β-Sr_2SiO_4 phase is the low temperature phase while α′-Sr_2SiO_4 phase the high temperature one[14]. There are two kinds of cation sites for Sr^{2+} in both α′ and β phases. Sr(Ⅰ) is ten-coordinated and Sr(Ⅱ) is nine-coordinated by oxygen atoms[15]. The amount of Sr(Ⅰ) site is equal to that of Sr(Ⅱ) site. For Sr(Ⅰ) site the average Sr—O bond distance is 0.285 2 nm in α′ phase and 0.285 0 nm in β phase. For Sr(Ⅱ) site the average Sr—O bond distance is 0.269 8 nm in α′ phase and 0.270 9 nm in β phase[16]. Since the ionic radius of the Ce^{3+} (0.125 nm, 10 coord.) is very similar to ionic radius of the Sr^{2+} (0.132 nm, 10 coord.), Ce^{3+} ions substitute Sr^{2+} ions in Sr_2SiO_4 lattice[17].

The commercial Sr_2SiO_4 phosphors are commonly produced by the conventional solid-state reaction method involving calcining at temperatures above 1 200 ℃[6-8]. Reports show that the synthesized temperature of the silicate phosphors can be lowered by using mesoporous silica as Si source[18-19]. In this paper, we synthesized $Sr_2SiO_4:Ce^{3+},Li^+$ phosphors at 1 000 or 1 100 ℃, using MCM-41 as silicon source. The relationships between emission property and Ce^{3+} concentration as well as Li^+ concentration are discussed. The influence of temperature on emission intensity is also studied.

2 Experiments

2.1 Preparation

MCM-41 was synthesized as follows: tetraethyl orthosilicate (TEOS) was added under constant stirring to a mixing solution of cetyltrimethylammonium bromide (CTAB), ammonia solution and distilled water. After stirred for 1 h at room temperature, the solution was sealed in a Teflon-lined stainless steel autoclave and heated at 110 ℃ for 48 h. The solid precipitate was filtered, washed, dried and calcined in air at 550 ℃ for 6 h. The molar ratio of the reactants was $n(CTAB):n(TEOS):n(NH_3\cdot H_2O):n(H_2O)=0.24:0.075:0.01:66.7$.

The $Sr_{2-x}SiO_4:xCe^{3+}$ ($x=0.01-0.09$, in steps of 0.01) and $Sr_{1.95-y}SiO_4:0.05Ce^{3+},yLi^+$ ($y=0.01-0.07$, in steps of 0.02) phosphors were prepared as follows: $Sr(NO_3)_2$, $LiNO_3$, and $Ce(NO_3)_3$ (0.1 mol/L) solution were mixed in deionized water to get a homogenized solution A. Amount of MCM-41 and oxalic acid (n(MCM-41):n(oxalic acid) = 1:1.5, molar ratio), ammonia solution was uniformly mixed in deionized water as solution B, sonicating for about 25 min. Then solution A was added dropwise to the solution B under vigorous stirring. After stirred for 1 h and then stilled at room temperature for 2 h, the products were filtered, washed, dried, and calcined at 1 000 or 1 100 ℃ for 3 h in the carbon reduction atmosphere.

2.2 Characterizations

X-ray powder diffraction (XRD) measurements were performed on the Rigaku D/MAX-Ultima S equipped with Cu Ka radiation (40 kV, 20 mA), at the rate of 2.0(°)/min over the range of 1°−8° (2θ), and 6.0(°)/min over the range of 20°−70°

(2θ). The particle morphology and size were measured using a thermal field emission electron microscope (SUPRA 55, Carl Zeiss, Germany) at an accelerating voltage of 3.00 kV. The excitation and emission spectra were measured on a FluoroMax-4 fluorescent spectrophotometer with a slit width of 0.8 nm and a Xe lamp as light source. The quantum efficiency was measured by a FluoroMax-4 fluorescent spectrophotometer. All the samples were measured at room temperature.

3 Results and Discussion

XRD pattern of MCM-41 powder is shown in Fig. 1. It can be observed that there are three well-resolved peaks at 2θ range of 1° – 5°, indexed as (100), (110) and (200) reflections of the hexagonal phase MCM-41[20]. This indicates that the synthesized sample possesses typical mesoporous structure of MCM-41.

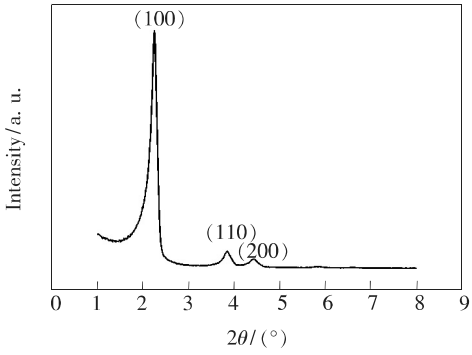

Fig. 1　XRD pattern of MCM-41

XRD patterns of $Sr_{2-x}SiO_4$: xCe^{3+} samples calcined at 1 100 ℃ are shown in Fig. 2. For x = 0.01 sample, major β-Sr_2SiO_4 phase co-exists with minor α′-Sr_2SiO_4 phase. When x increased to 0.03, the intensity of diffraction peaks of β-Sr_2SiO_4 decreased. When x is higher than 0.03, the β-Sr_2SiO_4 phase completely transforms into the pure α′-Sr_2SiO_4 phase, and a weak peak at 2θ = 28.6°, assigned to the (111) diffraction of the CeO_2 phase, can be clearly observed.

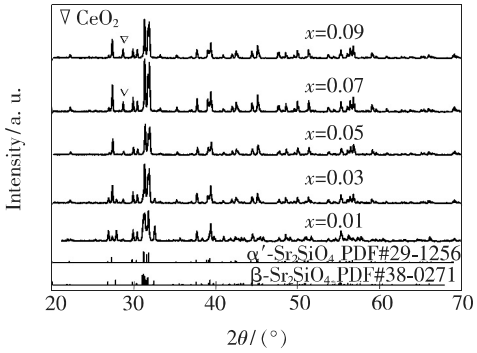

Fig. 2　XRD patterns of $Sr_{2-x}SiO_4$: xCe^{3+} samples calcined at 1 100 ℃

XRD patterns of $Sr_{1.95}SiO_4$: $0.05Ce^{3+}$ and $Sr_{1.9}SiO_4$: $0.05Ce^{3+}$, $0.05Li^+$ samples calcined at different temperatures are presented in Fig. 3. All the three samples consist of nearly pure α′-Sr_2SiO_4 phase with only minor CeO_2 impurity phase. Compared to the $Sr_{1.95}SiO_4$: $0.05Ce^{3+}$ sample calcined at 1 000 ℃, the diffraction peaks of $Sr_{1.95}SiO_4$: $0.05Ce^{3+}$ and $Sr_{1.9}SiO_4$: $0.05Ce^{3+}$, $0.05Li^+$ calcined at 1 100 ℃ shift to the higher angle-side, indicating the lattice shrinking with rising calcining temperature.

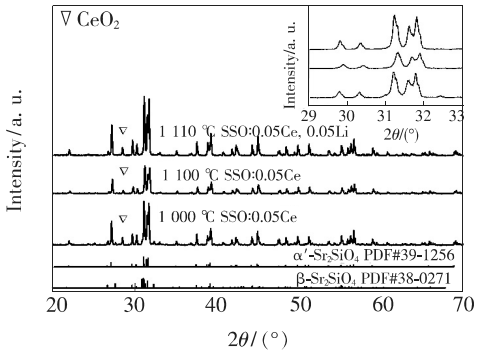

Fig. 3　XRD patterns of $Sr_{1.95}SiO_4$: $0.05Ce^{3+}$ and $Sr_{1.9}SiO_4$: $0.05Ce^{3+}$, $0.05Li^+$ samples calcined at different temperatures

The structure of α′-Sr_2SiO_4 is similar to that of β-K_2SiO_4 and has been described in literature[21-22]. The schematic crystal structure of α′-Sr_2SiO_4 phase is shown in Fig. 4(a). There are two cation sites of Sr^{2+} in α′-Sr_2SiO_4 phase. Sr(Ⅰ) is 10-coordinated and Sr(Ⅱ) is 9-coordinated by oxygen atoms, as shown in Fig. 4(b).

SEM images of $Sr_{1.95}SiO_4$: $0.05Ce^{3+}$ samples calcined at different temperatures are shown in Fig. 5. For samples calcined at 1 000 ℃, the particle diameters are about 2.3 μm and the shape is regular. As the calcining temperature increased from 1 000 ℃ to 1 100 ℃, the particle sizes increase from 2.3 μm to 4.2 μm, and the shape is also regular. Compared with the sample calcined at 1 000 ℃, the sample at

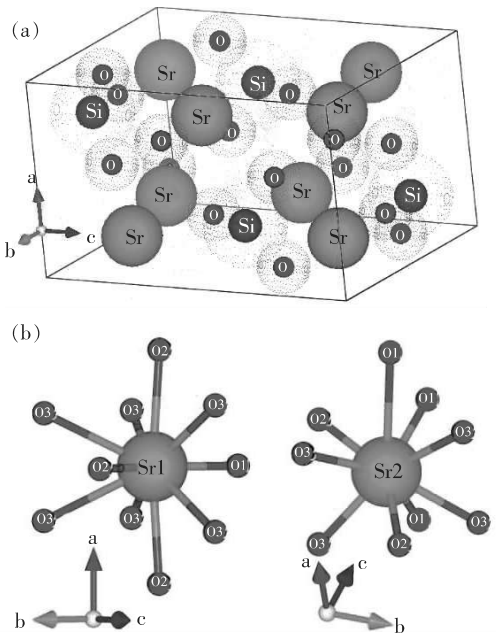

Fig. 4 (a) Schematic crystal structure of α′-Sr_2SiO_4 phase. (b) Coordination environments of Sr(Ⅰ) and Sr(Ⅱ) sites in α′ phase.

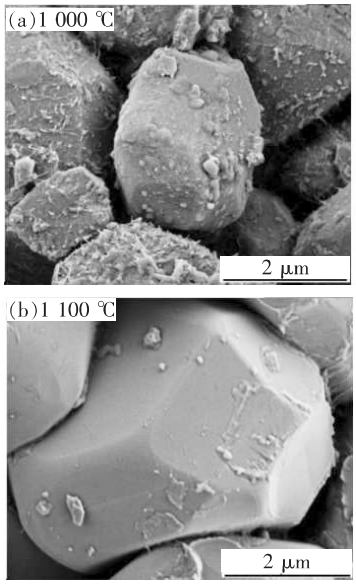

Fig. 5 SEM images of $Sr_{1.95}SiO_4$:0.05Ce^{3+} samples calcined at different temperatures

1 100 ℃ shows cleaner particle surfaces and more straight grain boundaries. It indicates that the sample calcined at 1 100 ℃ has better crystallinity.

Fig. 6 shows the emission and excitation spectra of the $Sr_{2-x}SiO_4$:xCe^{3+} samples calcined at 1 100 ℃. All the excitation spectra show two bands at about 280 nm and 351 nm, corresponding to the 4f-5d transition of Ce^{3+}. The emission spectra show an asymmetric broad band with a maximum locating at around 410 nm, ascribed to the 5d-4f transition of Ce^{3+}. The emission peak shifts towards red with increasing x. The emission intensity and half-band width increase significantly with increasing Ce^{3+} concentration, and gradually decrease as x exceeding 0.05. This shows that 5% Ce^{3+} is a critical concentration in Sr_2SiO_4.

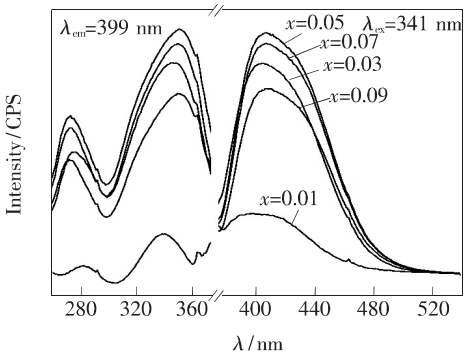

Fig. 6 Emission and excitation spectra of $Sr_{2-x}SiO_4$:xCe^{3+} samples calcined at 1 100 ℃

The emission spectrum of $Sr_{1.95}SiO_4$:0.05Ce^{3+} could be decomposed into two Gaussian peaks centered at 398 nm and 424 nm, respectively, as shown in Fig. 7. According to Van Uitert's empirical equation[23] shown below, the emission wavelength of Ce^{3+} in Sr_2SiO_4 host could be calculated to identify the sites of Ce^{3+} ions.

$$E = Q\left[1 - \left(\frac{V}{4}\right)^{\frac{1}{V}} 10^{-\frac{n\cdot ea\cdot r}{80}}\right], \qquad (1)$$

Q is the position in energy for the lower d-band edge for the free ion (50 000 cm^{-1} for Ce^{3+}). V is the valance of the activator, and is 3 for Ce^{3+} ion. n is the coordination number of the host cation. r is the radius of the host cation replaced by Ce^{3+} ion. ea is the electron affinity of the atoms that form anions

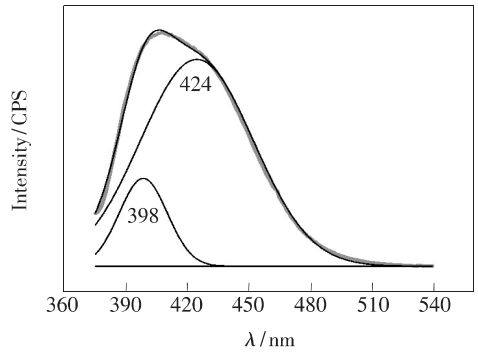

Fig. 7 Gaussian peak fittings for emission spectrum of $Sr_{1.95}SiO_4$: 0.05Ce^{3+} calcined at 1 100 ℃

(1.6 eV for O^{2-}). The ionic radius of 10- and 9-coordinated Sr^{2+} are 0.132 nm and 0.125 nm, respectively[16]. The calculated peaks of Ce^{3+} in ten-coordinated Sr(Ⅰ) and nine-coordinated Sr(Ⅱ) are located at 396 nm and 436 nm, respectively. The observed emission peaks at 398 nm and 424 nm are in very good agreement with the calculated peaks, and can be attributed to the Ce^{3+}(Ⅰ) and Ce^{3+}(Ⅱ), respectively. The result indicates that Ce^{3+} ions occupy the two different sites of Sr^{2+} in Sr_2SiO_4 host.

The Gaussian fitting results for the spectra of $Sr_{2-x}SiO_4:xCe^{3+}$ phosphors are summarized in Tab. 1. As shown in Tab. 1, when the content of Ce^{3+} increases in the range of 0.01 to 0.05, the ratio of integral area of Gaussian fitting peak Ce^{3+}(Ⅰ) to Ce^{3+}(Ⅱ) decreases, indicating a preference for Ce^{3+} to occupy the smaller Sr(Ⅱ) site rather than the larger Sr(Ⅰ) site in the solid solution. The radius of Ce^{3+} is smaller than that of Sr^{2+}. The preferent occupation of smaller Sr^{2+}(Ⅱ) by Ce^{3+} can reduce lattice distortion.

Tab. 1　Gaussian fitting results for the spectra of $Sr_{2-x}SiO_4:xCe^{3+}$ phosphors

Phosphors	Observed/nm		Ratio of area
	Ce(Ⅰ)	Ce(Ⅱ)	(Ce(Ⅰ)/Ce(Ⅱ))
$Sr_{1.99}SiO_4:0.01Ce^{3+}$	388	420	33/67
$Sr_{1.97}SiO_4:0.03Ce^{3+}$	395	423	22/78
$Sr_{1.95}SiO_4:0.05Ce^{3+}$	398	424	15/85
$Sr_{1.93}SiO_4:0.07Ce^{3+}$	398	424	15/85
$Sr_{1.91}SiO4:0.09Ce^{3+}$	398	426	18/82

The emission spectra of $Sr_{1.95}SiO_4:0.05Ce^{3+}$ and $Sr_{1.9}SiO_4:0.05Ce^{3+},0.05Li^+$ calcined at different temperatures are presented in Fig. 8. As the calcining temperature increased from 1 000 ℃ to 1 100 ℃, the emission intensities of phosphors enhance obviously. This can be attributed to the improved crystallinity. It can also be observed from Fig. 8 that the emission intensity of $Sr_{1.9}SiO_4:0.05Ce^{3+},0.05Li^+$ is much higher than that of $Sr_{1.95}SiO_4:0.05Ce^{3+}$ calcined at the same temperature. Doping Li^+ ions can obviously improve the emission intensity. The degree of improvement is influenced by the calcining temperature. Obviously, doping Li^+ ions improve the emission intensity of $Sr_{1.95}SiO_4:0.05Ce^{3+}$ calcined at 1 100 ℃ more effectively than that calcined at 1 000 ℃.

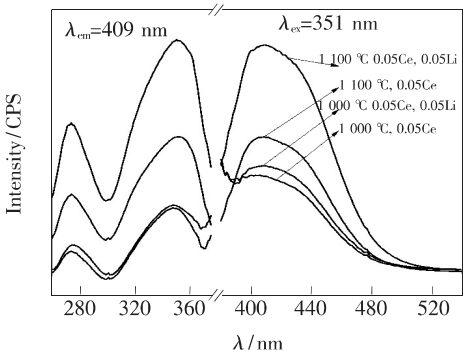

Fig. 8　Excitation and emission spectra of $Sr_{1.95}SiO_4:0.05Ce^{3+}$ and $Sr_{1.9}SiO_4:0.05Ce^{3+},0.05Li^+$ calcined at different temperatures

Fig. 9 shows the emission spectra of $Sr_{1.95-y}SiO_4:0.05Ce^{3+},yLi^+$ under 351 nm excitation. It can be seen that all the samples show the characteristic emission of Ce^{3+} at 410 nm and no distinct diversifications on the shapes and positions of the emission spectra are observed. The emission intensities of $Sr_{1.95-y}SiO_4:0.05Ce^{3+},yLi^+$ increase with increasing y, and gradually decrease as the doping concentration of Li^+ exceeds $y=0.05$. The intensity of sample with $y=0.05$ shows the highest intensity, two times as high as that of sample with $y=0$. The results indicate that the most suitable doping amount for Li^+ is equal to that for Ce^{3+}. The non-equivalent substitution of Sr^{2+} by Ce^{3+} can lead to the advent of Sr^{2+} vacancy, which acts as the charge trapping center and hence quenches the luminescence. When the monovalent alkali metal ion Li^+ is co-doped as the charge compensator, the number of the vacancies decreases with increasing concentration of Li^+, and the emission intensity is therefore improved[24-26].

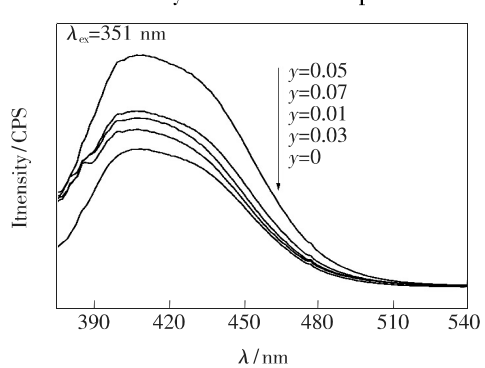

Fig. 9　Emission spectra of $Sr_{1.95-y}SiO_4:0.05Ce^{3+},yLi^+$

The internal quantum efficiency (IQE) was measured using the excitation source of 351 nm. The IQE of $Sr_{1.95}SiO_4:0.05Ce^{3+}$ and $Sr_{1.9}SiO_4:0.05Ce^{3+}$, $0.05Li^+$ calcined at 1 100 ℃ were obtained to be 23.7% and 35.7%, respectively. The result suggests that doping proper amount of Li^+ ions is an effective method to enhance the IQE of $Sr_2SiO_4:Ce^{3+}$ phosphor.

The measured chromaticity coordinates (x_c, y_c) of $Sr_{2-x-y}SiO_4:xCe^{3+},yLi^+$ phosphors are summarized in Tab. 2. The CIE chromaticity diagram of $Sr_{1.95-y}Li_ySiO_4:0.05Ce^{3+}$ phosphors is shown in Fig. 10. It can be seen that all the samples exhibit blue-purple emissions. The variation of Li^+ doping concentration only influences the emission intensity and has little effect on the colorimetric coordinate location in the CIE chromaticity diagram.

Tab. 2 Chromaticity coordinates (x_c, y_c) of $Sr_{2-x-y}SiO_4:xCe^{3+},yLi^+$ phosphors

Sample	x_c	y_c
$Sr_{1.99}SiO_4:0.01Ce^{3+}$	0.151 3	0.081 2
$Sr_{1.97}SiO_4:0.03Ce^{3+}$	0.156 7	0.037 5
$Sr_{1.95}SiO_4:0.05Ce^{3+}$	0.156 0	0.035 8
$Sr_{1.93}SiO_4:0.07Ce^{3+}$	0.155 8	0.037 8
$Sr_{1.91}SiO_4:0.09Ce^{3+}$	0.155 2	0.040 8
$Sr_{1.94}SiO_4:0.05Ce^{3+},0.01Li^+$	0.156 1	0.036 9
$Sr_{1.92}SiO_4:0.05Ce^{3+},0.03Li^+$	0.155 9	0.038 6
$Sr_{1.9}SiO_4:0.05Ce^{3+},0.05Li^+$	0.155 7	0.034 7
$Sr_{1.88}SiO_4:0.05Ce^{3+},0.07Li^+$	0.155 7	0.036 5

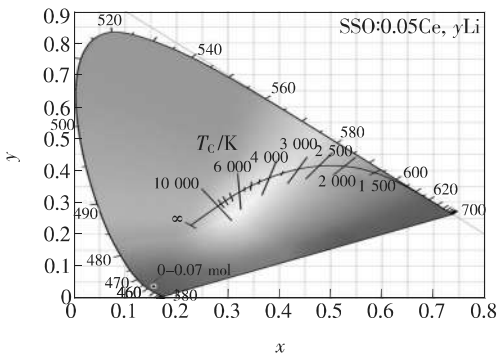

Fig. 10 CIE chromaticity coordinates of $Sr_{1.95-y}Li_ySiO_4:0.05Ce^{3+}$ phosphors

4 Conclusion

$Sr_{2-x}SiO_4:xCe^{3+}$ and $Sr_{1.95-y}SiO_4:0.05Ce^{3+},yLi^+$ phosphors have been prepared at 1 000 or 1 100 ℃. For $Sr_{2-x}SiO_4:xCe^{3+}$ samples, major β-Sr_2SiO_4 phase co-exists with minor α′-Sr_2SiO_4 phase when $x=0.01$, and the α′-Sr_2SiO_4 phase completely transforms into β-Sr_2SiO_4 phase when $x>0.03$. All the samples exhibit blue-purple emissions. The critical mole fraction of Ce^{3+} is found to be 5%. Doping proper amount of Li^+ ions can improve the emission intensity of $Sr_{1.95}SiO_4:0.05Ce^{3+}$ calcined at 1 100 ℃ more effectively than that at 1 000 ℃. The most suitable doping amount of Li^+ for $Sr_{1.95-y}SiO_4:0.05Ce^{3+},yLi^+$ is $y=0.05$. The results in present work could be helpful for efficiently enhancing the luminescence of $Sr_2SiO_4:Ce^{3+}$ phosphor.

References:

[1] LI Y Y, SHI Y R, ZHU G, *et al.*. A single-component white-emitting $CaSr_2Al_2O_6:Ce^{3+},Li^+,Mn^{2+}$ phosphor *via* energy transfer [J]. *Inorg. Chem.*, 2014, 53(14):7668-7675.

[2] HUANG C H, CHIU Y C, LIU W R. $Ca_3Si_2O_4N_2:Ce^{3+},Li^+$ phosphor for the generation of white-light-emitting diodes with excellent color rendering index values [J]. *Eur. J. Inorg. Chem.*, 2014, 2014(23):3674-3680.

[3] 雷炳富,沙磊,刘应亮,等. 纳米 $Sr_2SiO_4:Eu^{3+}$ 荧光粉的燃烧法合成及光谱性质 [J]. 发光学报, 2011, 32(6): 535-541.
LEI B F, SHA L, LIU Y L, *et al.*. Synthesis of nano-sized $Sr_2SiO_4:Eu^{3+}$ phosphor by combustion method and its luminescence properties [J]. *Chin. J. Lumin.*, 2011, 32(6):535-541. (in Chinese)

[4] CHEN J, LIU Y G, LIU H K, *et al.*. The luminescence properties of novel α-$Mg_2Al_4Si_5O_{18}:Eu^{2+}$ phosphor prepared in air [J]. *RSC Adv.*, 2014, 4(35):18234-18239.

[5] GUPTA S K, KUMAR M, NATARAJAN V, *et al.*. Optical properties of sol-gel derived $Sr_2SiO_4:Dy^{3+}$-photo and thermally stimulated luminescence [J]. *Opt. Mater.*, 2013, 35(12):2320-2328.

[6] ZHANG X G, TANG X P, ZHANG J L, *et al.*. An efficient and stable green phosphor $SrBaSiO_4:Eu^{2+}$ for light-emitting diodes [J]. *J. Lumin.*, 2010, 130(12):2288-2292.

[7] LEE S H, YOUNG H, KANG Y C, *et al*.. Characteristics of α′-and β-$Sr_2SiO_4:Eu^{2+}$ phosphor powders prepared by spray pyrolysis [J]. *Ceram. Int.*, 2010, 36(4):1233-1238.

[8] JU L C, CAI C, ZHU Q Q, *et al*.. Color tunable $Sr_2SiO_4:Eu^{2+}$ phosphors through the modification of crystal structure [J]. *J. Mater. Sci.: Mater. Electron.*, 2013, 24(11):4516-4521.

[9] SARADHI M P, LAKSHMINARASIMHAN N, BOUDIN S, *et al*.. Enhanced luminescence of $Sr_2SiO_4:Dy^{3+}$ by sensitization (Ce^{3+}/Eu^{2+}) and fabrication of white light-emitting-diodes [J]. *Mater. Lett.*, 2014, 117:302-304.

[10] GHILDIYAL R, HSU C H, LU C H. Aliovalent ion substitution and enhanced photoluminescence of $Sr_2SiO_4:Tb^{3+}/Z^+$ (Z = Li, Na, and K) phosphors [J]. *Int. J. Appl. Ceram. Technol.*, 2011, 8(4):759-765.

[11] SEKAR S, ARUNKUMAR P, JEYAKUMAR D, *et al*.. White light emission in alkali metal ion co-doped single host lattice phosphor $Sr_3B_2O_6:Ce^{3+},Eu^{2+},A^+$[$A$ = Li, Na and K] [J]. *Ceram. Int.*, 2015, 41(3):3497-3501.

[12] BRGOCH J, BORG C K H, DENAULT K A, *et al*.. Tuning luminescent properties through solid-solution in $(Ba_{1-x}Sr_x)_9Sc_2Si_6O_{24}:Ce^{3+},Li^+$ [J]. *Solid State Sci.*, 2013, 18:149-154.

[13] HA M G, HAN K R, KIM J S, *et al*.. Effects of incorporated alkali metal ions on the chemical bonding states and optical properties in $Sr_2SiO_4:Sm^{3+}$ phosphors [J]. *J. Korean Phy. Soc.*, 2014, 64(4):579-583.

[14] HAN J K, HANNAH M E, PIQUETTE A, *et al*.. Structure dependent luminescence characterization of green-yellow emitting $Sr_2SiO_4:Eu^{2+}$ phosphors for near UV LEDs [J]. *J. Lumin.*, 2012, 132(1):106-109.

[15] LEE J H, KIM Y J. Photoluminescent properties of $Sr_2SiO_4:Eu^{2+}$ phosphors prepared by solid-state reaction method [J]. *Mater. Sci. Eng.* B, 2008, 146(1-3):99-102.

[16] BARZOWSKA J, SZCZODROWSKI K, KROŚNICKI M, *et al*.. Influence of high pressure on $Sr_2SiO_4:Eu^{2+}$ luminescence [J]. *Opt. Mater.*, 2012, 34(12):2095-2100.

[17] LAKSHMINARASIMHAN N, VARADARAJU U V. White-light generation in $Sr_2SiO_4:Eu^{2+},Ce^{3+}$ under near-UV excitation a novel phosphor for solid-state lighting [J]. *J. Electrochem. Soc.*, 2005, 152(9):H152-H156.

[18] XIONG L M, SHI J L, GU J L, *et al*.. A mesoporous template route to the low-temperature preparation of efficient green light emitting Zn_2SiO_4: Mn phosphors [J]. *J. Phys. Chem.* B, 2005, 109(2):731-735.

[19] LU Q S, LI J G. Low-temperature synthesis of $Y_2SiO_5:Eu^{3+}$ powders using mesoporous silica and their luminescence properties [J]. *Opt. Mater.*, 2011, 33(3):381-384.

[20] BECK J S, VARTULI J C, ROTH W J, *et al*.. A new family of mesoporous molecular sieves prepared with liquid crystal templates [J]. *J. Am. Chem. Soc.*, 1992, 114(27):10834-10843.

[21] GUPTA S K, MOHAPATRA M, KAITY S, *et al*.. Structure and site selective luminescence of sol-gel derived Eu: Sr_2SiO_4 [J]. *J. Lumin.*, 2012, 132(6):1329-1338.

[22] CATTI M, GAZZONI G, IVALDI G. Structures of twinned β-Sr_2SiO_4 and of α′-$Sr_{1.9}Ba_{0.1}SiO_4$ [J]. *Acta Cryst.*, 1983, 39(1):29-34.

[23] VAN UITERT L G. An empirical relation fitting the position in energy of the lower d-band edge for Eu^{2+} or Ce^{3+} in various compounds [J]. *J. Lumin.*, 1984, 29(1):1-9.

[24] TIAN L H, MHO S I. Enhanced luminescence of $SrTiO_3:Pr^{3+}$ by incorporation of Li^+ ion [J]. *Solid State Commun.*, 2003, 125(11-12):647-651.

[25] WU H Y, HU Y H, ZHANG W, *et al*.. Flux's influence on the luminescent properties of europium and dysprosium co-doped melilite long afterglow phosphor [J]. *J. Non-Cryst. Solids*, 2012, 358(20):2734-2740.

[26] GAWANDE A B, SONEKAR R P, OMANWAR S K. Synthesis and enhancement of luminescence intensity by co-doping of M^+ (M = Li, Na, K) in Ce^{3+} doped strontium haloborate [J]. *Opt. Mater.*, 2014, 36(7):1143-1145.

游静(1990 –),女,福建漳州人,硕士研究生,2013 年于昆明理工大学获得学士学位,主要从事稀土掺杂硅酸盐基质发光材料方面的研究。
E-mail: youjing186@126.com

李湘祁(1968 –),女,湖南宜章人,副教授,1990 年于中南工业大学(现中南大学)获得博士学位,主要从事介孔材料、硅酸盐基质发光材料的合成应用方面的研究。
E-mail: lxiangqi@fzu.edu.cn